Earthquakes and Structures, *Vol. 15, No. 5 (2018) 453-462*
DOI: https://doi.org/10.12989/eas.2018.15.5.453

Evaluation of seismic performance of mid-rise reinforced concrete frames subjected to far-field and near-field ground motions

Mokhtar Ansari*[1], Masoud Ansari[2a] and Amir Safiey[3b]

[1]*Department of Civil Engineering, Bozorgmehr University of Qaenat, Qaen, Iran*
[2]*Department of Civil Engineering, Semnan University, Semnan, Iran*
[3]*Glenn Department of Civil Engineering, Clemson University, Clemson, SC, USA*

(Received November 1, 2017, Revised August 2, 2018, Accepted August 7, 2018)

Abstract. Damages to buildings affected by a near-fault strong ground motion are largely attributed to the vertical component of the earthquake resulting in column failures, which could lead to disproportionate building catastrophic collapse in a progressive fashion. Recently, considerable interests are awakening to study effects of earthquake vertical components on structural responses. In this study, detailed modeling and time-history analyses of a 12-story code-conforming reinforced concrete moment frame building carrying the gravity loads, and exposed to once only the horizontal component of, and second time simultaneously the horizontal and vertical components of an ensemble of far-field and near-field earthquakes are conducted. Structural responses inclusive of tension, compression and its fluctuations in columns, the ratio of shear demand to capacity in columns and peak mid-span moment demand in beams are compared with and without the presence of the vertical component of earthquake records. The influences of the existence of earthquake vertical component in both exterior and interior spans are separately studied. Thereafter, the correlation between the increase of demands induced by the vertical component of the earthquake and the ratio of a set of earthquake record characteristic parameters is investigated. It is shown that uplift initiation and the magnitude of tensile forces developed in corner columns are relatively more critical. Presence of vertical component of earthquake leads to a drop in minimum compressive force and initiation of tension in columns. The magnitude of this reduction in the most critical case is recorded on average 84% under near-fault ground motions. Besides, the presence of earthquake vertical components increases the shear capacity required in columns, which is at most 31%. In the best case, a direct correlation of 95% between the increase of the maximum compressive force and the ratio of vertical to horizontal 'effective peak acceleration (EPA)' is observed.

Keywords: earthquake vertical component; reinforced concrete; moment resisting frames; axial column force; shear capacity; near-fault earthquake; statistical correlation

1. Introduction

Earthquakes shake buildings in a three-dimensional manner. In recent decades, the influence of horizontal shakings of the earthquake on buildings had been extensively investigated. Seismic design provisions are fundamentally geared to account for horizontal components of ground motions. In practice, the vertical component of an earthquake is mostly neglected except in special cases in the building design as elaborated in typical model codes, e.g., CEN (2005) and FEMA 356 (2000). Additionally, the vertical component is taken as a fraction of the horizontal ground motion, which sometimes turns out very unrealistic. The vertical ground accelerations in an earthquake are known to reach or even exceed the horizontal accelerations. This could cause unreliable predictions of the structure behavior because of lack of a solid grasp of the vertical component of seismic shaking as well as the vertical behavior of the structure. Moreover, seismic hazard assessment studies hardly take the vertical component of the earthquake into consideration. (FEMA 356 2000, Bisch, *et al.* 2012, Eleftheriadou and Karabinis 2012, Cao and Ronagh 2014, Bas and Kalkan 2016)

This research is devoted to studying comparatively the effects of vertical components of the earthquake on seismic behavior of reinforced concrete moment resisting frames excited by both far- and near-fault earthquakes. Different key seismic parameters of structural response, and their sensitivities and correlations with the vertical component of the earthquake are also studied.

A relatively short distance between the source of the earthquake (i.e., rupture) and the location of the building precludes dissipations of high frequencies leading to an acceleration time history with high-frequency content. Also, it is well established that near-fault earthquake record entails a stronger vertical component in comparison to far-fault ones. The vertical component of an earthquake usually contains a relatively lesser amount of energy. However, earthquake vertical component tends to release its energy in a narrow frequency domain. This makes buildings with

*Corresponding author, Assistant Professor
E-mail: ansari@buqaen.ac.ir
[a]MSc.
E-mail: ansari@buqaen.ac.ir
[b]Research Assistant
E-mail: asafiey@g.clemson.edu

ISSN: 2092-7614 (Print), 2092-7622 (Online)

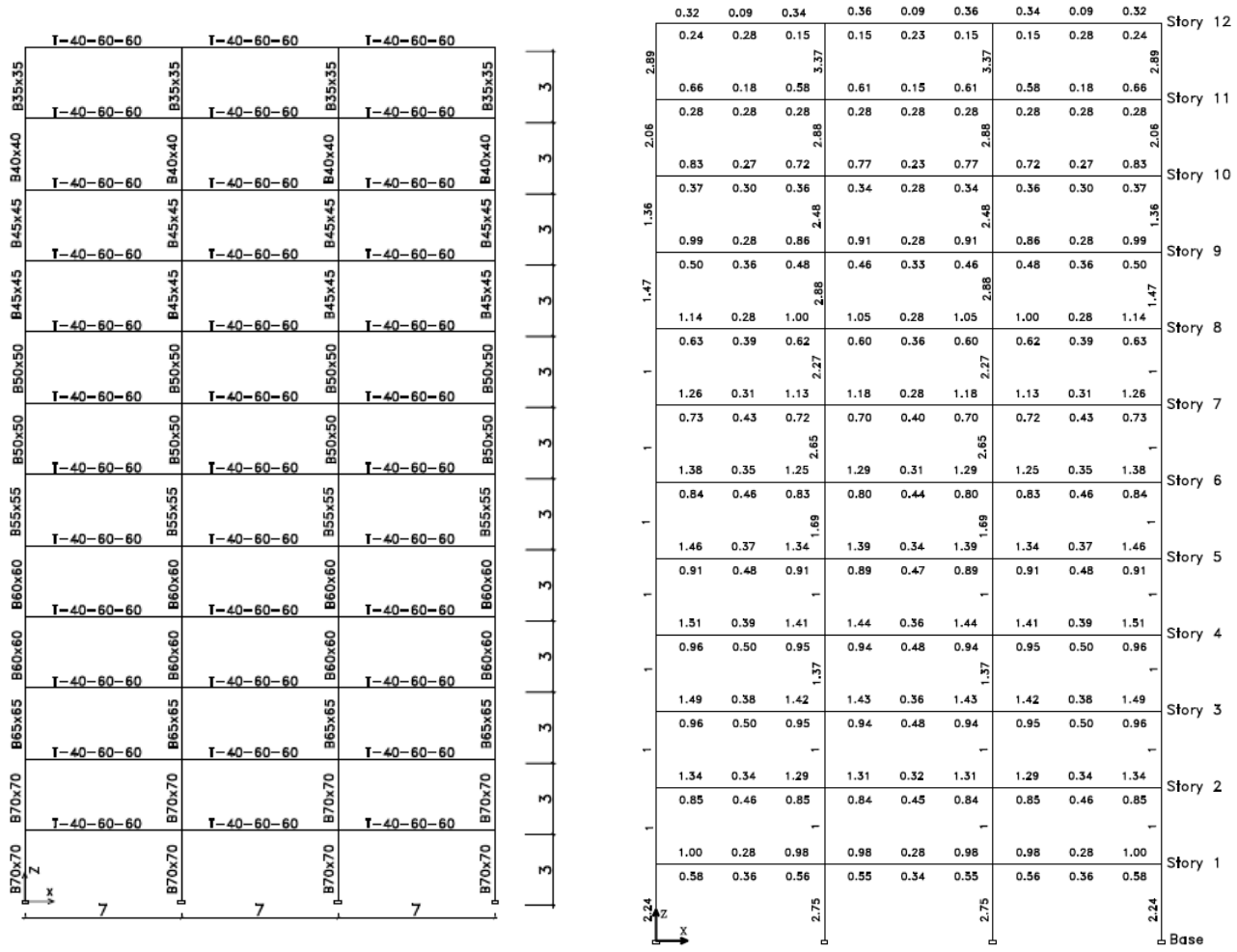

Fig. 1 Sizing and percent of reinforcing of archetype members

vertical periods of vibration, which lie within this earthquake vibration domain, to damage severely. Lower damping of the building structure in vertical direction plays an important role well. (Somerville and Graves 1993, Somerville 1997, Collier and Elnashai 2001, Esfahanian and Aghakouchak 2015, Eskandari *et al.* 2017) Other factors also play a salient role in the formation of seismic shaking with strong vertical component including not dissipating amplitude and constant frequency content of the vertical component in contrast to horizontal one due to inelastic behavior soil of site, shallow depth of epicenter and reverse faulting. (Mohamrnadioun and Pecker 1984, Aguirre and Irikura 1995, Ambraseys and Simpson 1995, Mayes and Shaw 1997, Papageorgiou 1998, Rigato and Medina 2007, Kim *et al.* 2011, Rejec *et al.* 2012, Bayraktar and Altunişik 2014, Ghaffarzadeh and Nazeri 2015, Losanno *et al.* 2017, Mohammadi *et al.* 2017)

Having observed destructive damages occurred in buildings in previous earthquakes attributable to the vertical component of the earthquake, plenty of studies defined around the subject. In 1995, Papazoghlou defined a parameter named ‘stiffness ratio’. This includes generation of 2% damping of minimum and maximum response spectrum of a column idealized as a single degree freedom system for different values of stiffness ratio, initial axial load, and vertical excitation. This shows the development of tensile force under different circumstances. Furthermore, one corrective method was proposed to modify structural response in case of development of tension in columns to account for different stiffness in a column in tension and compression. (Elnashai and Papazoglou 1995, Elnashai and Papazoglou 1997) Broderick *et al.* (1994) conducted a research on the axial load developed in columns exposed to vertical excitation. It was concluded, in the first mode of vertical vibration, the variation of axial load is higher in columns and walls located in upper stories. In addition, middle columns are more vulnerable than external ones. (Broderick 1994, Tajammolian *et al.* 2014, Zhai *et al*. 2016, Mazza *et al.* 2017)

Collier and Elnashai (2001) studied the vertical vibration period of buildings under earthquake vertical component. The study includes maximum acceleration of vertical component, the lag phase between the maximum of vertical and horizontal acceleration components and domain of maximum horizontal component. These are important parameters tend to elongate vertical vibration period. It was concluded that all these three parameters make vibration period elongate at different levels. (Collier and Elnashai 2001)

In addition, Di Sarno *et al.* (2011) studied seismic

performance reinforced concrete members due to vertical and horizontal components of a suite of four near-fault earthquake records of L'Aquila earthquake. Key parameters of the study include normalized axial force in beam-column members and the ratio of the maximum magnitude of horizontal to vertical components of the earthquake. The result reveals an increase of axial force fluctuation in columns and development of residual deformations in columns due to the presence of a strong vertical component of the earthquake. Furthermore, the shear response was significantly influenced by the combination of the horizontal and vertical earthquake ground component. (Di Sarno *et al.* 2011)

Most of the previous studies are devoted to studying the behavior of a single column under the vertical component of the earthquake. This paper investigates how the presence of the vertical component of the earthquake can influence internal forces of members of a code-complying reinforced concrete moment frame. Moreover, a sensitivity and correlation study is conducted to understand interdependencies between internal demands.

2. Archetype

Archetype under study is a 12-story reinforced concrete moment frame with three bays each one spanning 7 m. This represents a perimeter frame of a symmetrical building with space reinforced concrete special moment frame. Building details including member sizes and reinforcing are presented on Fig. 1. It is designed in accordance with ACI 318-14 with the spectral acceleration of 0.35 g and soil type of '*D*'. (ACI 2014) ZeusNL software is adopted to handle nonlinear simulation of the structure. (Elnashai *et al*. 2006) Floor gravity load carrying system is the slab-beam system. Beams are considered *T*-shape in the modeling. *T-a-b-c* means a beam with *T*-shape and web thickness *a*, total height *b* and flange width *c*, all in cm. Flange thickness for all beams are constant and equal to 15 cm. Baxb represents column members in which *a* and *b* are the column width and depth, respectively. Percent of Longitudinal reinforcement of members are shown in Fig. 1. Loading to the model is applied in both concentrated and distributed manners. Concentrated loading is employed to investigate the axial load in the columns. Distributed loading is used to study moment at beams' mid-span and the ratio of shear demand and capacity of columns. Table 1 explains concentrated and distributed loadings as implemented in ZeusNL.

The nonlinear dynamic is carried out under two sets of near and far-fault earthquake records, each set consisting of 9 records. Considering the limitation of two-dimensional analysis, vertical component and horizontal component perpendicular to the fault of near-fault earthquake records and vertical component plus larger horizontal component of far-fault earthquake records are adopted. Each near-fault earthquake record corresponds to one far-fault earthquake record representing the same event but from different distances. Records are scaled in a way that entails the same maximum horizontal acceleration of 0.35 g, and maintains the same magnitude of maximum horizontal to the vertical component of earthquake ratios before and after scaling. Table 2 presents more details about earthquake records. A similar study for 3, 6 and 9-story frames is conducted revealing the very similar result. The nonlinear model is corroborated by an experimental study carried out by Kim and Elnashai (2008).

Table 1 Model gravity loading

Dead load	4 kN/m^2
Live Load	2 kN/m^2
Beam distributed mass	0.0045 N.S^2/mm^2
Concentrated mass on top of the corner column	907575 N.S^2/mm
Concentrated mass on top of the middle column	1204 N.S^2/mm

Table 2 Earthquake records characteristics

Rec. No.	Earthquake Name	Year	Mn	Closest Distance (km)	H1 Scaled PGA (g)	V Scaled PGA (g)
Far-fault						
f1	Morgan Hill	1984	6.19	31.88	0.35	0.14
f2	Loma Prieta	1989	6.93	41.03	0.35	0.15
f3	Loma Prieta	1989	6.93	44.11	0.35	0.13
f4	Northridge-01 1994-01-17 12:31	1994	6.69	57.51	0.35	0.28
f5	Northridge-01 1994-01-17 12:31	1994	6.69	53.94	0.35	0.19
f6	Northridge-01 1994-01-17 12:32	1994	6.69	59.62	0.35	0.09
f7	Chi-Chi, Taiwan 1999-09-20	1999	7.62	28.17	0.35	0.22
f8	Chi-Chi, Taiwan 1999-09-20	1999	7.62	44.76	0.35	0.09
f9	Chi-Chi, Taiwan 1999-09-20	1999	7.62	41.67	0.35	0.17
Mean					0.35	0.16
Near-fault						
n1	Morgan Hill	1984	6.19	0.53	0.35	0.17
n2	Loma Prieta	1989	6.93	9.96	0.35	0.23
n3	Loma Prieta	1989	6.93	3.88	0.35	0.32
n4	Northridge-01	1994	6.69	5.43	0.35	0.56
n5	Northridge-01	1994	6.69	5.43	0.35	0.56
n6	Northridge-01	1994	6.69	5.19	0.35	0.16
n7	Chi-Chi, Taiwan	1999	7.62	3.14	0.35	0.16
n8	Chi-Chi, Taiwan	1999	7.62	2.76	0.35	0.31
n9	Chi-Chi, Taiwan	1999	7.62	9.35	0.35	0.38
Mean				5.07	0.35	0.32

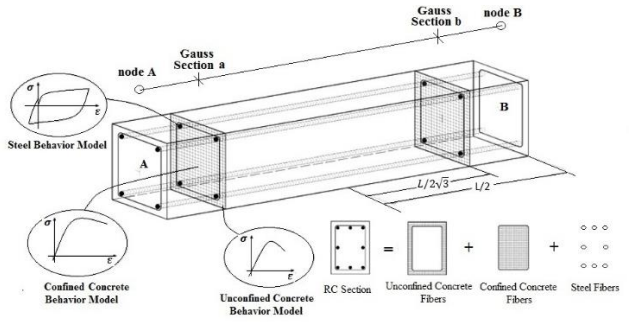

Fig. 2 Schematic presentation of modeling approaches adopted for reinforced concrete members to predict their nonlinear behavior (after Di Sarno *et al.* 2011)

2.1 Modelling of reinforced concrete members using fiber element

ZeusNL program is able to predict large displacements happened in three-dimensional frames under dynamic and static loadings including geometric and material nonlinearities. (Elnashai *et al.* 2006) Expansion of nonlinear behavior along the length and depth of the member can be modeled by proper discretization of the member into a set of elements and the cross-section into a network of fibers. This facilitates relatively to achieve the precise damage distribution. Distributed plasticity approach is adopted which can take into account the distribution of plasticity throughout the member. (Elnashai and Di Sarno 2008) The displacement-based beam-column element is undertaken. The behavior of reinforced concrete members can be more effectively predicted using distributed plasticity approach (Filippou and Issa 1988, Taucer *et al.* 1991, Filippou *et al.* 1992, Spacone *et al.* 1996, Kwak *et al.* 1997). This can take into account nonlinearity through the member contrasting to phenomenological approaches. This approach models the member behavior using weighted integration. In the implementation, only the behavior of some fibers in integration points is investigated. Deformations and forces are the primary unknowns in the member. Local forces and displacements are mapped onto global displacements and forces using shape functions. In this study, distributed plasticity and nonlinear displacement based beam-column elements with Gaussian Legendre integration method to model the nonlinear behavior of reinforced concrete members are employed.

3. Results

Nonlinear dynamic analyses under different suites of earthquake records are conducted with/without the presence of the vertical component of the earthquake. Maximum compressive axial load, maximum tensile axial force, fluctuations in axial loads, the maximum moment at mid-span of beams and ratio of shear demand to the capacity of columns and their variations in presence of earthquake vertical component is traced and studied.

3.1 Column axial forces

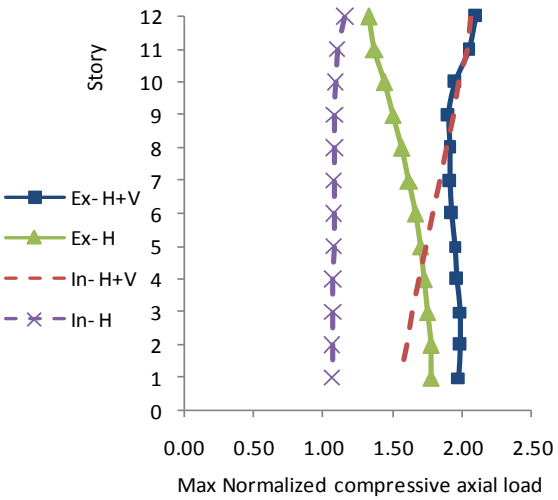

Fig. 3 Maximum mean compressive axial loads developed in columns due to near-fault earthquakes

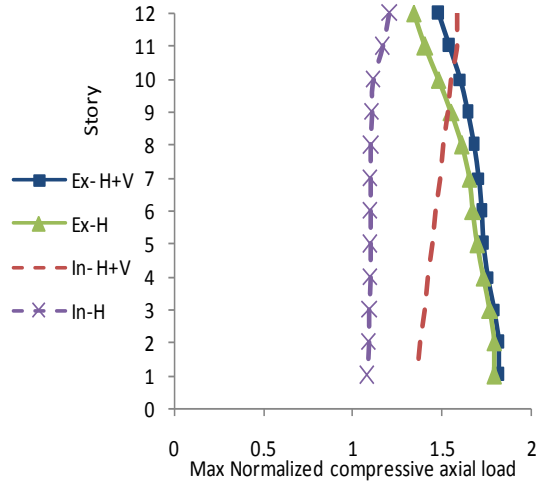

Fig. 4 Maximum mean compressive axial loads developed in columns due to far-fault earthquakes

Fig. 3 and Fig. 4 present compressive axial forces normalized to gravity load for different middle and external columns due to near-fault and far-fault earthquake records. It is a common practice amongst researchers to normalize the axial load of columns to gravity load. These figures suggest the presence of the vertical component of earthquake leads to increase of axial loads in columns. The increase is more significant in middle columns of upper floors. Also, this increase is more significant under near-fault excitations.

Fig. 5 and Fig. 6 present Minimum compressive axial forces normalized to gravity load for middle and external columns due to near-fault and far-fault earthquake records. These figures suggest the absolute value of compression is lower in external columns. However, the decline of axial compressive load similar and initiation of uplift, similar to compression case, is more critical in interior columns in upper stories under near-fault earthquakes.

Figs. 7 and 8 show fluctuations in axial load normalized to gravity load of interior and exterior columns due to near- and far-fault earthquakes. A similar trend observed which is

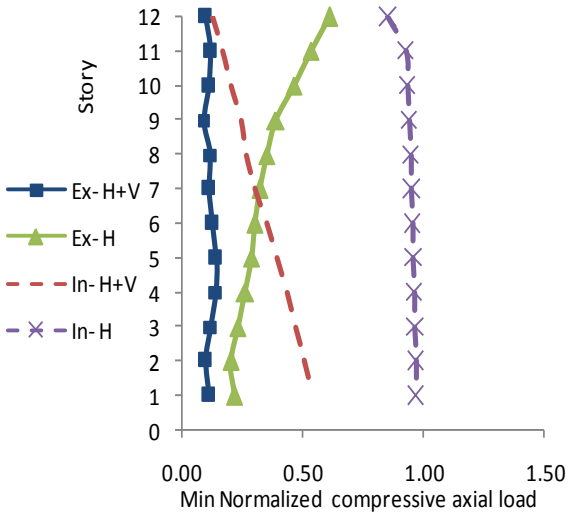

Fig. 5 Minimum mean compressive axial loads developed in columns due to near-fault earthquakes

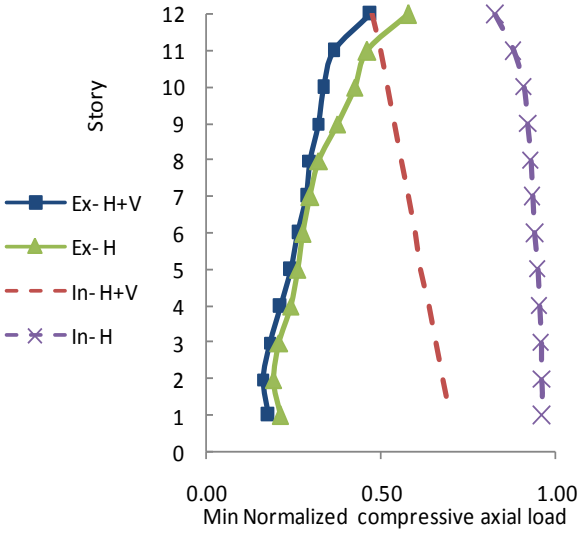

Fig. 6 Minimum mean compressive axial loads developed in columns due to far-fault earthquakes

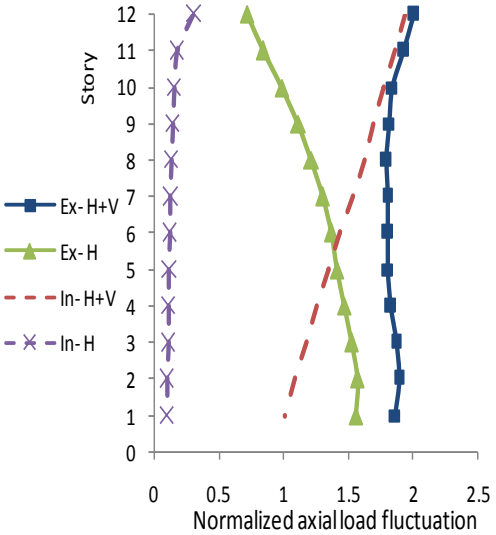

Fig. 7 Axial load fluctuations under near-fault earthquake records

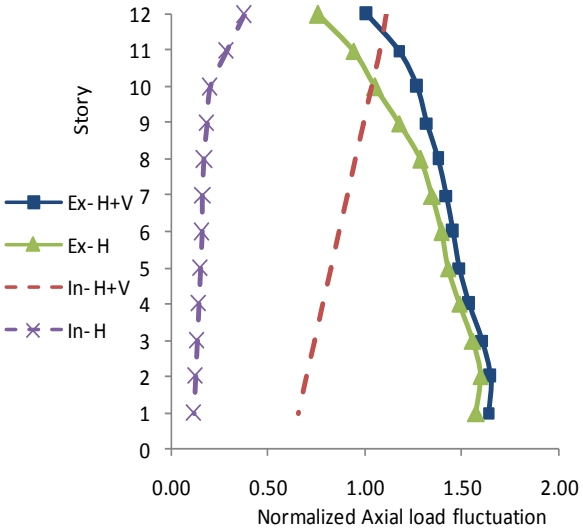

Fig. 8 Axial load fluctuations under far-fault earthquake records

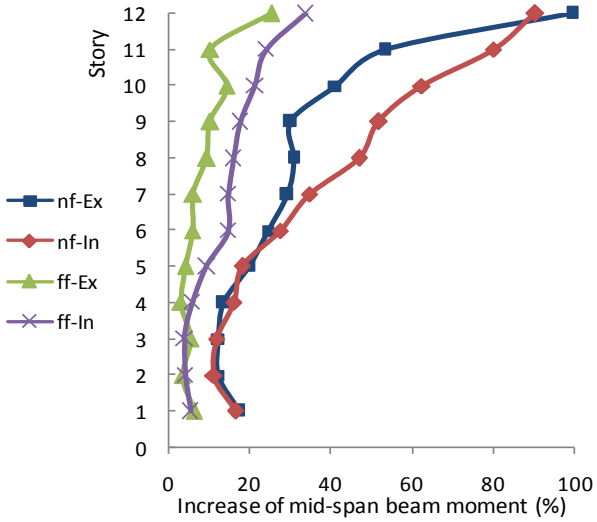

Fig. 9 Percentage of increase of mid-span beam moment

a higher increase of fluctuations in interior columns of upper stories under near-fault earthquakes is observed.

Fig. 9 illustrates mid-span moment normalized to corresponding mid-span gravity moment in different stories and interior or exterior spans developed due to near- and far -fault ground motions. This also further validates the previous results as to higher increase in beams in middle spans of upper stories under near-fault ground motions.

Demand to capacity ratio of shear (hereafter shear DCR) is studied for interior and exterior columns. Shear capacity of reinforced concrete column interacts with the member axial load. Shear capacity consists of the contribution of stirrups and concrete. Column sizing is enough to have concrete resisted internal shears in columns. However, the minimum stirrups as code mandates are provided. Code requirements are as follows (ACI 2014)

$$V_c = \left(1 + \frac{N_U}{14.A_g}\right)\left(\frac{\sqrt{f'_c}}{6}\right)(b_w.d) \qquad (1)$$

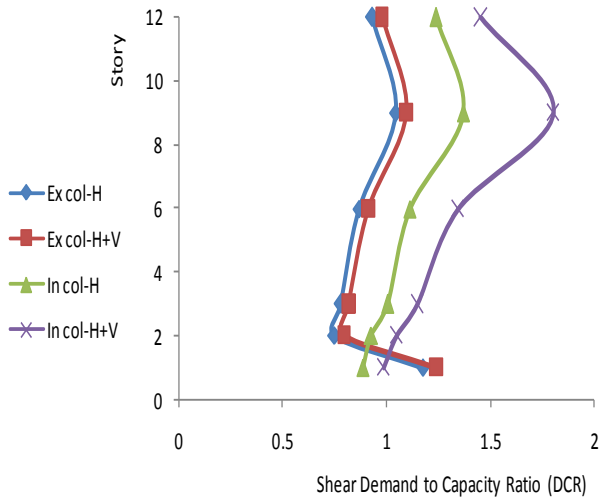

Fig. 10 Shear demand to capacity ratio under near-fault earthquakes

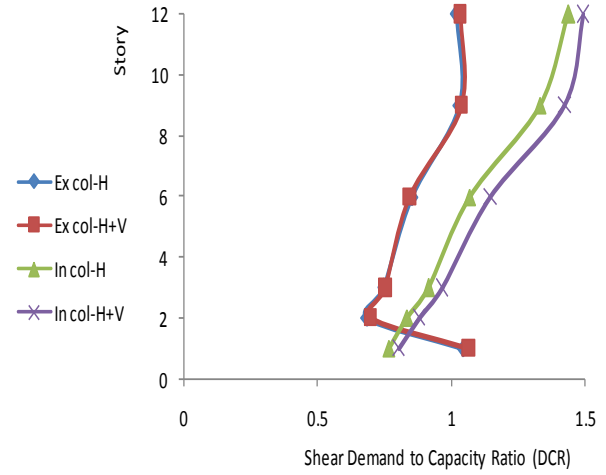

Fig. 11 Shear demand to capacity ratio under far-fault earthquakes

$$V_c = \left(1 + \frac{0.3.N_U}{A_g}\right)\left(\frac{\sqrt{f'_c}}{6}\right)(b_w.d) \geq 0 \qquad (2)$$

$$V_s)_{min} = \left(\frac{A_v}{s}\right)_{min}.f_y.d = \frac{1}{16}.\left(\sqrt{f'_c}\right)(b_w.d) \qquad (3)$$

Eq. (1) deals with concrete shear capacity under compression axial load, while Eq. (2) provides concrete shear capacity under tensile axial load. Eq. (3) presents the minimum necessary reinforcement. Compression is assumed to be positive, while tension is assumed to be negative. All units are in N and mm.

The ratio of maximum shear demand to the minimum capacity in the frame columns including middle and corner columns using the above formulas as well as the result of nonlinear dynamic analysis results under excitations with and without the vertical component of ground motion is obtained as plotted on Figs. 10 and 11.

3.2 Sensitivity and correlation study

Yet, study result proves higher vulnerability of interior columns in upper stories under near-fault earthquakes. In this section, correlation and sensitivity of influence of vertical component of earthquake record in these members against various parameters of vertical and horizontal components of the records is investigated. This includes an investigation over the ratio of different parameters of vertical to horizontal components of the earthquake. This means the calculation of increase of response in any specific member due to any ordered pair of vertical and horizontal components of earthquake record separately. In return, the ratio of vertical to horizontal components of different parameters is organized as ordered pairs and plotted. A line is fitted to the data along with the calculation of corresponding square Pearson correlation factor. The slope of the line shows the sensitivity of response to the parameter in question, and the correlation factor shows the goodness of linear regression. Eq. (4) describes Pearson correlation factor

$$R^2 = (Pearson\ Correlation\ Coefficient)^2 = \left(\frac{\sum[(x_i - \bar{x}).(y_i - \bar{y})]}{\sqrt{\sum(x_i - \bar{x})^2.\sum(y_i - \bar{y})^2}}\right)^2 \qquad (4)$$

To study the correlation and sensitivity of axial force responses and shear demand to capacity ratio, internal columns of the twelfth story is chosen. Similarly, internal beams of the same story are chosen to study correlation and sensitivity of mid-span moment.

There are five responses chosen including maximum and minimum column axial forces, fluctuations in axial loads, mid-span moment and the ratio of shear demand to capacity. Parameters characterizing the records under study are PGA, PGV, PGD, IV, ID, EPA and EPV.

PGA, PGV, and PGD are peak ground acceleration, velocity and displacement, respectively. IV and ID denote the area beneath greatest acceleration and displacement pulses, which are being calculated using relationships (5) and (6). EPA and EPV are being calculated from velocity and acceleration response spectrum using Eqs. (7) and (8)

$$IV = \max_{i=1,..,n}\left(\int_{t_i}^{t_{i+1}} a_g(t).dt\right) \qquad (5)$$

$$ID = \max_{i=1,..,n}\left(\int_{t_i}^{t_{i+1}} V_g(t).dt\right) \qquad (6)$$

$$EPA = \frac{\left(\int_{0.1}^{0.5} S_a(T).dT\right)}{2.5.(0.5-1)} \qquad (7)$$

$$EPV = \frac{\left(\int_{0.8}^{1.2} S_v(T).dT\right)}{2.5.(1.2-0.8)} \qquad (8)$$

In Eqs. (5) to (8), t_i represents the intersection point with time axis. $a_g(t)$ and $v_g(t)$ is acceleration and velocity records in terms of cm/sec and cm^2/sec, respectively. EPA and $S_a(T)$ units are cm/sec^2 and $S_v(T)$ unit is cm/sec.

Table 3 presents the ratio of vertical to horizontal components of record parameters under consideration.

Table 3 Horizontal to vertical ratio of different parameters for each earthquake record

	V/H (PGA)	V/H (PGV)	V/H (PGD)	V/H (IV)	V/H (ID)	V/H (EPA)	V/H (EPV)
n1	0.481101	0.250339	0.263203	0.22697	0.287727	0.261299	0.233894
n2	0.649647	0.390726	0.883631	0.323435	1.144078	0.304627	0.301044
n3	0.914088	0.710112	1.07106	0.305538	1.371039	0.41823	0.370846
n4	1.597452	0.467884	0.349245	0.310102	0.302529	0.608734	0.39994
n5	1.597223	0.468223	0.34377	0.309645	0.3022	0.60869	0.400564
n6	0.456314	0.213116	0.182295	0.139169	0.184974	0.300924	0.559867
n7	0.461916	0.468134	0.892434	0.282055	0.857847	0.220352	0.411451
n8	0.8964	0.501795	0.516873	0.785714	0.512524	0.559674	1.024214
n9	1.075455	0.97627	0.768968	1.53108	0.790306	0.452338	1.303262
f1	0.410714	0.331435	0.199178	0.355213	0.295681	0.335596	0.37043
f2	0.43	0.463695	0.36372	0.460006	0.364993	0.488701	0.327597
f3	0.364808	0.27581	0.430278	0.290461	0.559182	0.294659	0.381328
f4	0.795286	0.496917	0.413053	0.585346	0.492208	0.736506	0.689775
f5	0.550613	0.732415	0.331668	1.005096	0.443583	0.759965	0.482794
f6	0.269579	0.20958	0.300951	0.230197	0.265102	0.292891	0.200075
f7	0.617303	0.582539	0.726811	0.430483	0.75755	0.466836	0.550086
f8	0.255586	0.503874	1.182235	0.506029	1.139722	0.303045	0.653882
f9	0.478973	0.650823	0.678623	0.421612	0.793522	0.582098	0.524398

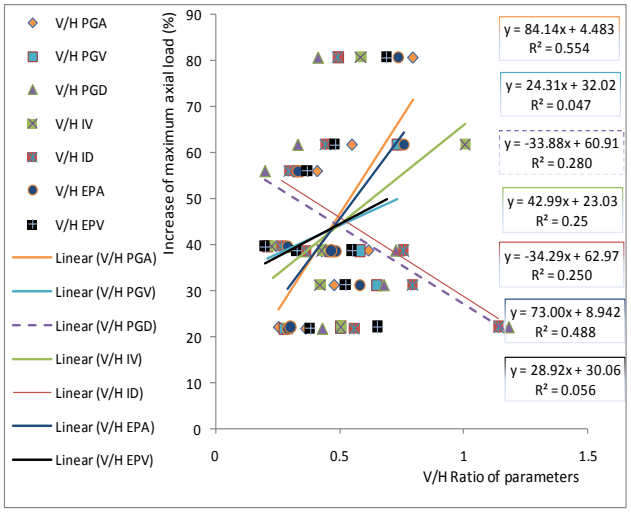

Fig. 12 Correlation between the influence of vertical earthquake components in increase of maximum axial load in columns with ratio of horizontal to vertical parameters of different near-fault earthquake record

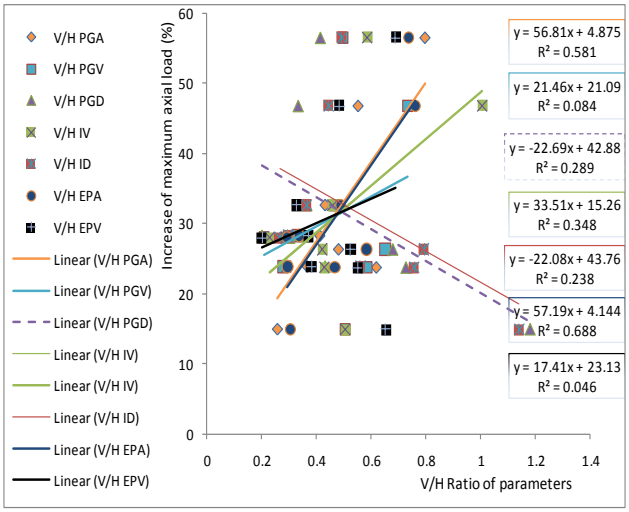

Fig. 13 Correlation between the influence of vertical earthquake components in increase of maximum axial load in columns with ratio of horizontal to vertical parameters of different far-fault earthquake record

Figs. 12 and 13 present respectively percentage of correlation and sensitivity between increases of the maximum axial load with the ratio of vertical to horizontal components of parameters under study for near- and far-fault earthquakes.

These figures suggest the maximum correlation of maximum compressive axial load increase is obtained with proportion to horizontal to the vertical component of PGA and EPA. Parameters describing displacement (e.g., PGD and ID) shows the second highest negative correlation after acceleration dependent parameters. Velocity-dependent parameters exhibit the least correlation. One can conclude these parameters are independent of an increase in responses under study. Moreover, the maximum sensitivity is observed for maximum axial compressive response with acceleration dependent parameters.

Table 4 Correlation matrix of increase of responses versus different near-fault earthquake record parameters

	PGA	PGV	PGD	IV	ID	EPA	EPV
F_N (max)	0.88	0.21	-0.4	0.31	-0.44	0.95	0.37
F_N (min)	0.89	0.12	-0.51	0.15	-0.55	0.89	0.23
ΔF_N	0.87	0.09	-0.47	0.06	-0.49	0.93	0.18
M (max)	0.93	0.13	-0.43	0.09	-0.47	0.84	0.07
Shear DCR	0.89	0.11	-0.44	0.17	-0.52	0.86	0.18

All plots are not presented here due to the limitation on the length. Correlation coefficient and slope of the fitted line is presented separately in two matrices (namely,

Table 5 Correlation matrix of increase of responses versus different far-fault earthquake record parameters

	PGA	PGV	PGD	IV	ID	EPA	EPV
F_N (max)	0.76	0.29	-0.54	0.59	-0.49	0.83	0.21
F_N (min)	0.74	0.22	-0.53	0.50	-0.50	0.70	0.24
ΔF_N	0.19	0.05	-0.50	0.34	-0.59	0.44	-0.33
M (max)	0.98	0.55	-0.22	0.59	-0.13	0.87	0.55
Shear DCR	0.87	0.13	-0.32	0.18	-0.29	0.54	0.36

Table 6 Sensitivity matrix of increase of responses versus different near-fault earthquake record parameters

	PGA	PGV	PGD	IV	ID	EPA	EPV
F_N (max)	72.49	34.85	-45.91	26.42	-38.92	233.7	38.05
F_N (min)	77.79	21.26	-62.8	13.73	-50.98	232.8	24.67
ΔF_N	590.30	119.5	-442.20	46.92	-356.4	1885.0	157.2
M (max)	130.90	35.39	-85.29	13.43	-70.79	352.3	13.47
Shear DCR	31.02	7.8	-21.25	6.12	-19.25	89.39	7.95

Table 7 Sensitivity matrix of increase of responses versus different far-fault earthquake record parameters

	PGA	PGV	PGD	IV	ID	EPA	EPV
F_N (max)	56.81	21.46	-22.69	33.51	-22.08	57.19	17.41
F_N (min)	84.14	24.31	-33.88	42.99	-34.29	73.0	28.92
ΔF_N	88.96	28.28	-128.0	118.90	-162.8	187.5	-165.4
M (max)	93.14	51.63	-12.1	42.31	-7.73	76.29	56.82
Shear DCR	12.39	1.92	-2.59	1.92	-2.53	7.03	5.47

correlation and sensitivity matrices) for two cases of near- and far-fault earthquakes.

Tables 4 and 5 presents the correlation of increase of responses against the ratio of vertical to horizontal components of parameters under study for near and far-fault earthquakes, respectively.

Tables 6 and 7 presents the sensitivity of increase of responses against the ratio of vertical to horizontal components of earthquake record parameters under study (which is the slope of the fitted line) for near and far-fault earthquakes, respectively.

Tables 4 and 5 suggest that the greatest correlation, in all cases, take place for parameters related to acceleration (EPA and PGA). In the second place, parameters related to displacement display the second highest negative correlation. Parameters related to velocity show the lowest correlation. The increase of these parameters can be assumed to be independent of an increase in response.

Tables 6 and 7 reveal that the greatest sensitivity is observed in parameters related to acceleration. Parameters related to displacement, with regard to their inverse correlation, similarly exhibits negative sensitivity. Velocity-dependent parameters showing the lowest correlation in all cases except one exhibiting positive sensitivity and correlation.

4. Conclusions

Column plays a key role in load carrying system of a building, which its failure can lead to the collapse of the building in a progressive collapse fashion. These members are prone to be vulnerable to the vertical component of the earthquake. Nonlinear dynamic analyses under different suites of ground motions with and without vertical earthquake component are carried out. Tensile axial load, compressive axial load, fluctuation in axial load, demand to capacity ratio of column shear and beam mid-span moment is studied and influence of the presence of the vertical component of an earthquake is identified. Furthermore, the sensitivity and correlation of obtained responses considering different parameters of the vertical and horizontal earthquake record are investigated, and could be summarized as follows:

The vertical component of an earthquake increases the axial load developed in columns dramatically which is more severe in case of near-fault earthquakes.

In upper stories, the percentage of difference in maximum axial load which is representing vertical earthquake component effect is higher.

In all studied cases, the presence of a vertical component of earthquake always increases compression, tension, axial load fluctuation, demand to capacity ratio of shear and beam mid-span moment leading to a more critical condition for the structure. Also, it was shown for all responses under consideration, response increases due to the presence of vertical component are more critical in middle spans and upper stories, and for near-field excitations.

A correlation study of response increases due to the vertical component of earthquake against the ratio of vertical to the horizontal component of various earthquake record parameters show acceleration dependent parameters are more correlated. In highest one, correlation of increase of maximum column compressive force with the ratio of the vertical to horizontal component of EPA is 0.95 and corresponding sensitivity is 233%.

Parameters related to displacement showed negative correlation for all cases, but they proved higher correlation compared to velocity-dependent parameters. Velocity-dependent parameters showed the least correlation.

Parameters related to acceleration exhibited the greatest slope and sensitivity. This means this has the highest effect on the increase of axial force response. The slope of parameters related to displacement was negative. This means by the increase of the ratio of vertical to horizontal components of these two parameters, the influence of vertical component of the earthquake on axial force response dwindles. The correlation of PGA and EPA under near-fault earthquake was larger compared to far-field ground motions.

Velocity-dependent parameters showed inconsequential correlation, however in all cases except one, exhibits positive slope. This means by an increase of the ratio of the horizontal to the vertical component of these parameters, the percentage of increase of axial responses increase.

References

ACI 318 (2014), Building Code Requirements for Structural Concrete and Commentary, American Concrete Institue, Farmington Hills, MI, USA.

Aguirre, J. and Irikura, K. (1995), "Preliminary analysis of non-linear site effects at port island vertical array station during the 1995 Hyogoken-Nambu earthquake", *J. Nat. Disast. Sci.*, **16**(2), 49-58.

Ambraseys, N.N. and Simpson, K.A. (1995), "Prediction of vertical response spectra in Europe", Research Report ESEE-95/1, Imperial College, London, UK.

Bas, S. and Kalkan, I. (2016), "The effects of vertical earthquake motion on an R/C structure", *Struct. Eng. Mech.*, **59**(4), 719-737.

Bayraktar, A., Altunişik A.C., Türker, T., Karadeniz H., Erdoğdu, Ş., Angın, Z. and Özşahin T.Ş. (2014), "Structural performance evaluation of 90 RC buildings collapsed during the 2011 Van, Turkey, Earthquakes", *J. Perform. Constr. Facil.*, **29**(6), 410-440.

Bisch, P., Carvalho, E., Degee, H. F., Fardis, M., F. P., Kreslin, and M. and Tsionis, G. (2012), "Eurocode 8: seismic design of buildings worked examples", Luxembourg: JRC Technical Report, Publications Office of European Union/Joint Research Center.

Broderick, B.M., Elnashai, A.S., Ambraseys, N.N., Barr, J., Goodfellow, R. and Higazy, M. (1994), "The Northridge (California) earthquake of 17 October 1994, observations, strong-motion and correlative response analyses", Report No. ESEE 4/94, Engineering Seismology and Earthquake Engineering, London.

Cao, V.V. and Ronagh, M.R. (2014), "Correlation between parameters of pulse-type motions and damage of low-rise RC frames", *Earthq. Struct.*, **7**(3), 365-384.

CEN (2005) European Standard EN 1998-1: 2005 Eurocode 8: Design of Structures for Earthquake Resistance, Part 1: General Rules, Seismic Action and Rules for Buildings, European Committee for Standardization, Brussels, Belgium.

Collier, C. and Elnashai, A. (2001), "A procedure for combining vertical and horizontal seismic action effects", *J. Earthq. Eng.*, **5**(4), 521-539.

Di Sarno, L., Elnashai, A. and Manfredi, G. (2011), "Assessment of RC columns subjected to horizontal and vertical ground motions recorded during the 2009 L'Aquila (Italy) earthquake", *Eng. Struct.*, **33**(5), 1514-1535.

Eleftheriadou, A.K. and Karabinis, A.I. (2012), "Seismic vulnerability assessment of buildings based on damage data after a NEAR FIELD earthquake (7 September 1999 Athens - Greece)", *Earthq. Struct.*, **3**(2), 117-140.

Elnashai, A. and Papazoglou, A. (1995), "Vertical earthquake ground motion-evidence, effects and simplified analysis procedures", Research Report ESEE-95/6, Imperial College, London.

Elnashai, A., Papanikolaou, V. and Lee, D. (2006), ZEUS-NL User Manual Version 1.7, Mid-America Earthquake Center, University of Illinois at Urbana-Champaign.

Elnashai, A.S. and Di Sarno, L. (2008), *Fundamentals of Earthquake Engineering*, Wiley and Sons, UK.

Elnashai, A.S. and Papazoglou, A.J. (1997), "Procedure and spectra for analysis of RC structures subjected to strong vertical earthquake loads", *J. Earthq. Eng.*, **1**(1), 121-155.

Esfahanian, A. and Aghakouchak, A.A. (2015), "On the improvement of inelastic displacement demands for near-fault ground motions considering various faulting mechanisms", *Earthq. Struct.*, **9**(3), 673-698.

Eskandari, R., Vafaei, D., Vafaei, J. and Shemshadian, M.E. (2017), "Nonlinear static and dynamic behavior of reinforced concrete steel-braced frames", *Earthq. Struct.*, **12**(2), 191-200.

FEMA 356 (2000), Prestandard and Commentary for the Seismic Rehabilitation of Buildings, Washington, D.C.

Ghaffarzadeh, H. and Nazeri, A. (2015), "The effect of the vertical excitation on horizontal response of structures", *Earthq. Struct.*, **9**(3), 625-637.

Kim, S.J. and Elnashai, A.S. (2008), "Seismic assessment of RC structures considering vertical ground motion", MAE Center Report, No. 08-03.

Kim, S.J., Holub, C.J. and Elnashai, A.S. (2011), "Analytical assessment of the effect of vertical earthquake motion on RC bridge piers", *J. Struct. Eng.*, ASCE, **137**(2), 252-260.

Losanno, D., Hadad, A.H. and Serino, G. (2017), "Seismic behavior of isolated bridges with additional damping under far-FIELD and NEAR fault ground motion", *Earthq. Struct.*, **13**(2), 119-130.

Maddaloni, G., Magliulo, G. and Cosenza, E. (2012), "Effect of the seismic input on non-linear response of R/C building structures", *Adv. Struct. Eng.*, **15**(10), 1861-1877.

MAE Center (2017), MAECENTER, Retrieved from ZEUS-NL: http://mae.cee.illinois.edu/software/software_zeusnl.html

Mayes, R. and Shaw, A. (1997), "The effect of near fault ground motion on bridge columns", *Proceedings of the FHWA/NCEER Workshop on the National Representation of Seismic*, Buffalo, N.Y.

Mazza, F., Mazza, M. and Vulcano, A, (2017), "Nonlinear response of R.C. framed buildings retrofitted by different base-isolation systems under horizontal and vertical components of near-fault earthquakes", *Earthq. Struct.*, **12**(1), 135-144.

Mohammadi, M.H., Massumi, A. and Meshkat-Dini, A. (2017), "Performance of RC moment frames with fixed and hinged supports under near-fault ground motions", *Earthq. Struct.*, **13**(1), 89-101.

Mohamrnadioun, B. and Pecker, A. (1984), "Low-frequency transfer of seismic energy by superficial soil deposits and soft rocks", *Earthq. Eng. Struct. Dyn*, **12**(4), 537-564.

Papageorgiou, A. (1998), "The character of near source ground motion and related seismic design issues", *Proceedings of the Structural Engineers Word Congress*, San Francisco, CA.

Rejec, K., Isaković, T. and Fischinger, M. (2012), "Seismic shear force magnification in RC cantilever structural walls, designed according to Eurocode 8", *Bull. Earthq. Eng.*, **10**(2), 567-586.

Rigato, A.B. and Medina, R.A. (2007), "Influence of angle of incidence on seismic demands for inelastic single story structures subjected to bi-directional ground motions", *Eng. Struct.*, **29**(10), 2593-2601.

Somerville, P. (1997), "The characteristics and Quantification of near fault ground motions", FHWA/NCEER Workshop on the National Representation of Seismic, Buffalo, N.Y.

Somerville, P. and Graves, R. (1993), "Conditions that give rise to unusually large long period ground motion", *Struct. Des. Tall Build.*, **2**(3), 211-232.

Tajammolian, H., Khoshnoudian, F., Talaei, S. and Loghman, V. (2014), "The effects of peak ground velocity of NEAR-FIELD ground motions on the seismic responses of base-isolated structures mounted on friction bearings", *Earthq. Struct.*, **7**(6), 1259-1282.

Zhai, C.H., Zheng, Z., Li, S., Pan, X. and Xie, L.L. (2016), "Seismic response of nonstructural components considering the near-fault pulse-like ground motions", *Earthq. Struct.*, **10**(5), 1213-1232.

CC

Acronyms

PGA: Peak ground acceleration
PGV: Peak ground velocity
PGD: Peak ground Displacement
IV: Incremental velocity
ID: Incremental Displacement
EPA: Effective peak acceleration
EPV: Effective peak velocity